A. Supplementary Material

A1. Artifact removal

We used the multivariate exploratory linear optimized decomposition tool (MELODIC; Beckmann and Smith, 2014) to decompose our raw BOLD signal into independent components (IC). IC-based strategy for motion artifact removal have been shown to be more reliable to remove motion-induced signal variations than regression from motion parameters (Pruim et al., 2015). Two researchers independently hand classified a sample of 20 participants' IC into two categories: 'clear artifact' (e.g., motion/deglutition, susceptibility, or blood flow in arteries) or 'potential signal'. Labels were then compared between the two judges, where each discrepancy was discussed until an agreement was reached (inter-rater reliability = 93%). Manually classified components obtained by this process were used to train a classifier using random forest machine learning algorithm. Leave-one-out testing—where we iteratively left one participant out of the training and tested the classifier accuracy on the left-out participant—at the optimal sensitivity resulted in a median 94% true positive rate (i.e., the percentage of 'true signal' accurately classified). Consequently, we applied the FMRIB's ICA-based X-noiseifier (FIX) to automatize the denoising of our BOLD signal (Salimi-Khorshidi et al., 2014).

Supplementary Figures and Tables

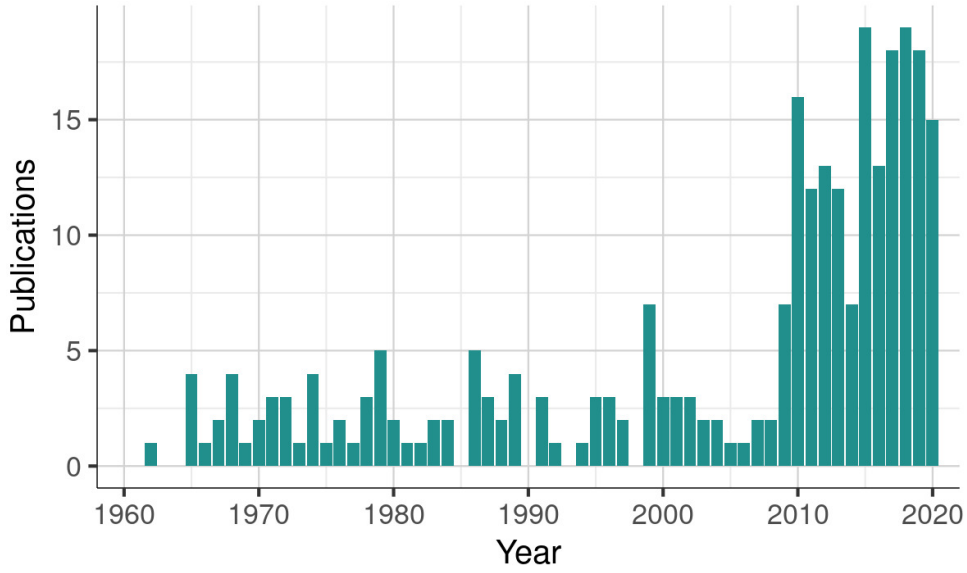

Figure S1: **Publications listed on Google Scholar.** Results returned when queried with the search terms involving a 'gustometer'. Results show a clear increase of the number of publication over the years, culminating with over 300 publications in 2020.

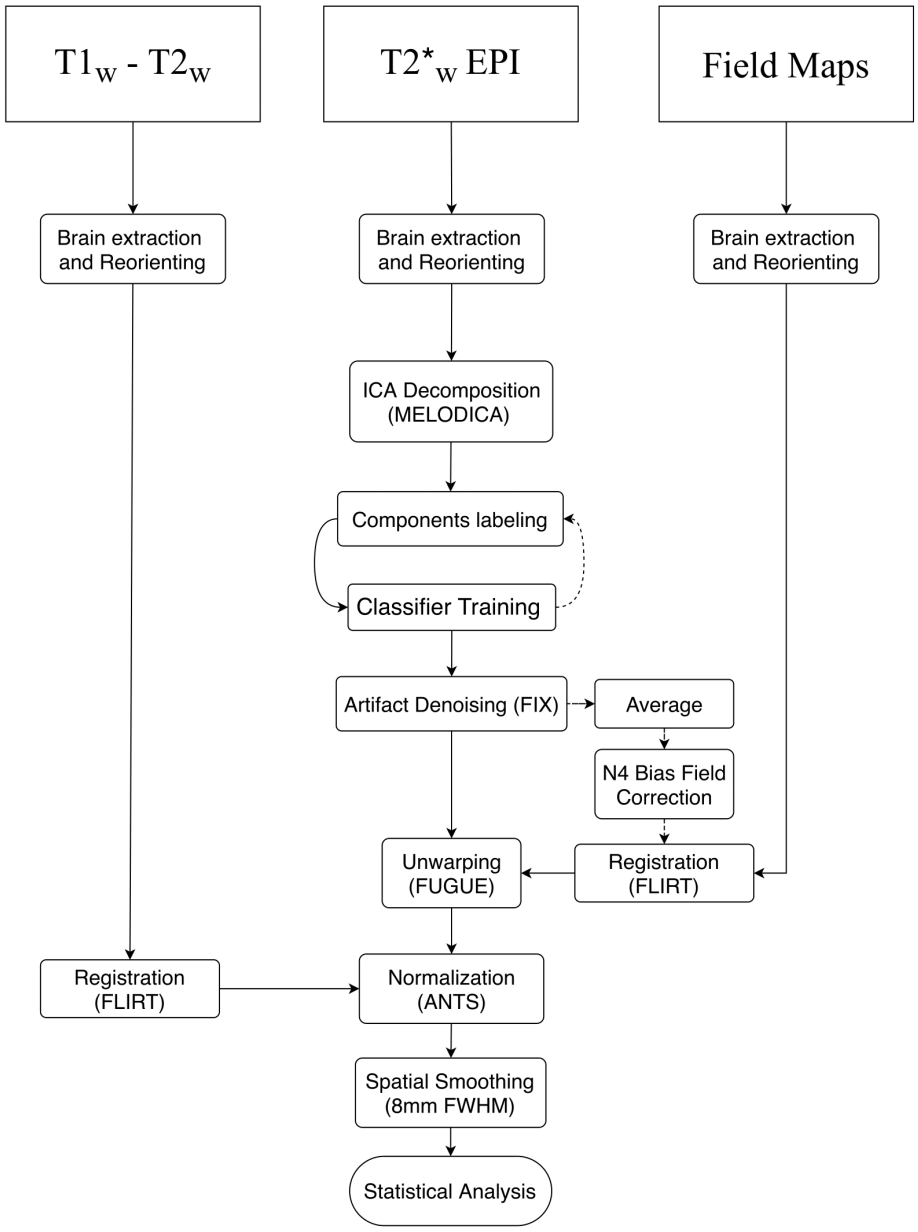

Figure S2: **Flow chart representation of the preprocessing pipeline**. Custom-built pipeline to improve the removal of deglutition artifacts in functional MRI.

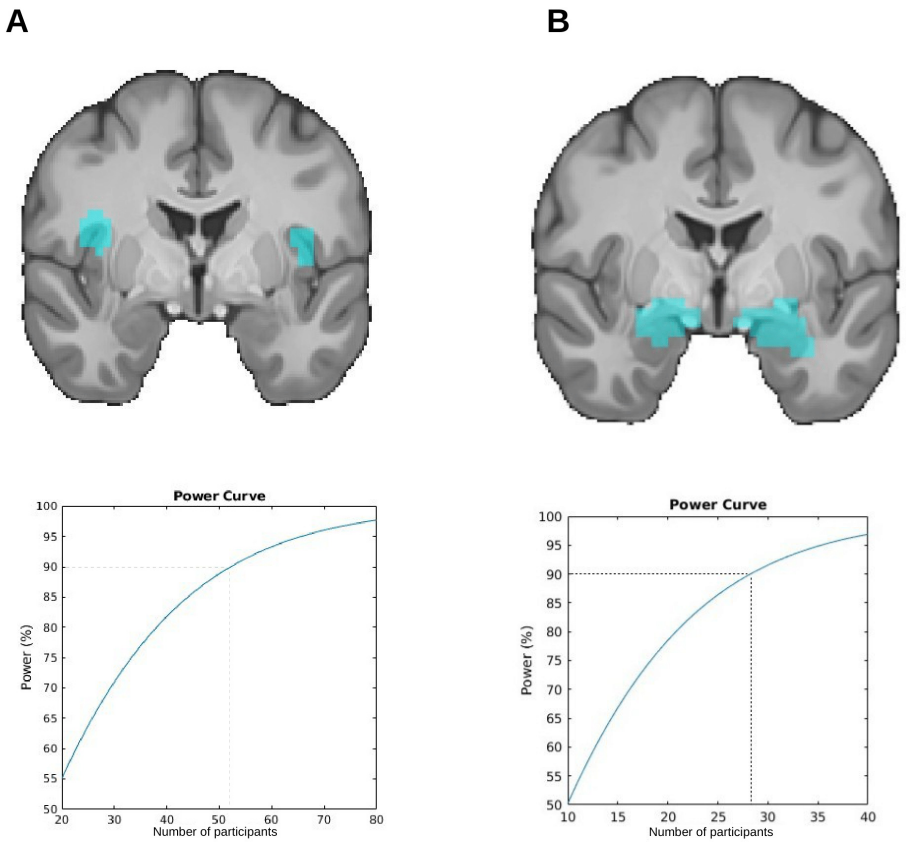

Figure S3: **Observed power. (A)** One would need 53 participants to reproduce our results within the insular cortex with a power of 90% and an $\alpha = 0.05$. **(B)** One would need 29 participants to reproduce our results within the piriform cortex.

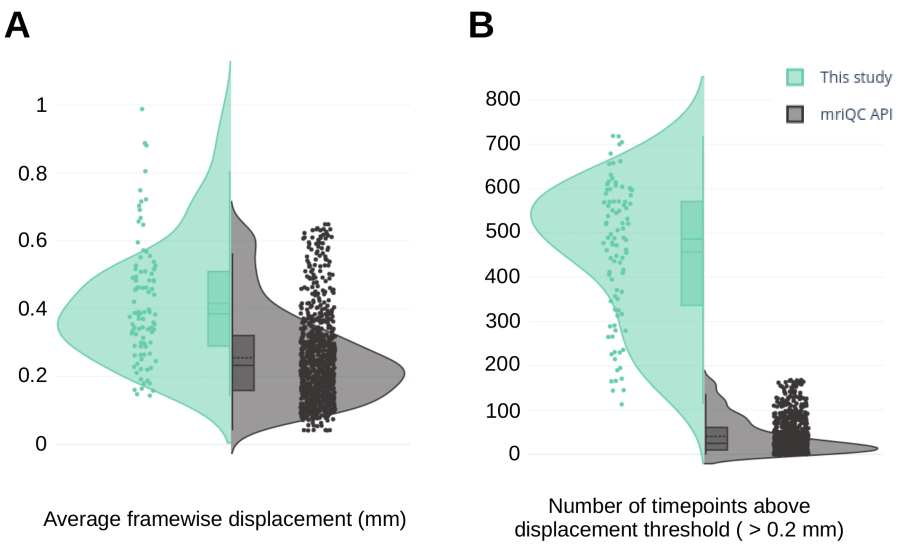

Figure S4: **Framewise displacement compared to normative data**. **(A)** Average framewise displacement (FD) from each time series compared to 834 crowd-sourced data points with similar scanner parameters from the magnetic resonance imaging quality check (MRIQC) Web-API (mriqc.nimh.nih.gov). The average FD is calculated as the displacement on the surface of a sphere (Power et al., 2012). **(B)** Number of timepoints above FD threshold compared to the MRIQC Web-API.

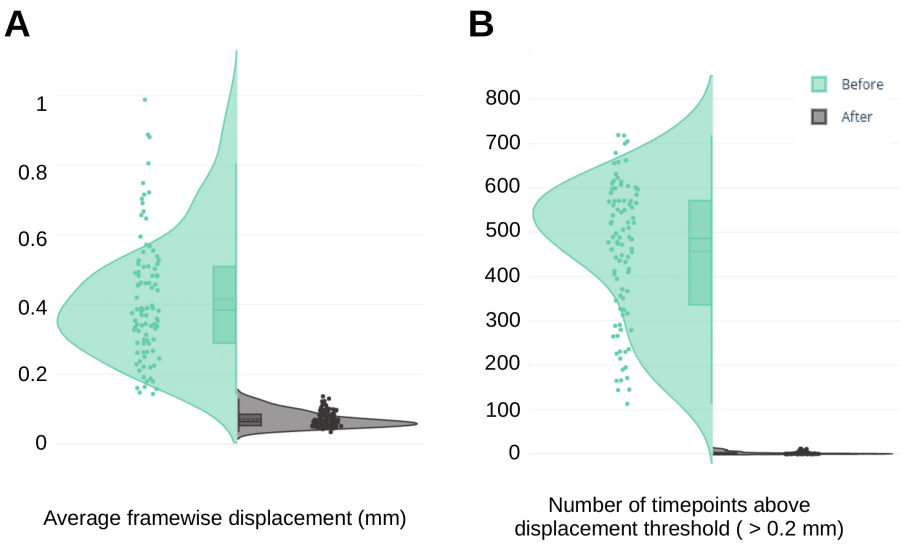

Figure S5: **Framewise displacement compared before and after preprocessing**. **(A)** Average framewise displacement (FD) from each time series compared to the same time series after artifact removal (see A1 for more information). The average FD is calculated as the displacement on the surface of a sphere (Power et al., 2012). **(B)** Number of timepoints above FD threshold compared to the same time series after artifact removal.

Table S1: Summary Results of the intensity ratings

Effect	μ	SE	Statistic (t)	Df	p-value	Effect size (d_z)	95% CI
condition	30.33	2.5	12.40	84	< 0.001	1.35	1.04 – 1.63

References

Beckmann, C. F. and Smith, S.M.(2004). Probabilistic independent component analysis for functional magnetic resonance imaging. *IEEE Transactions on Medical Imaging*, 23(2):137–152.

Power, J. D., Barnes, K. A., Snyder, A. Z., Schlaggar, B. L., and Petersen, S. E. (2012). Spurious but systematic correlations in functional connectivity MRI networks arise from subject motion. *NeuroImage*, 59(3):2142-2154.

Pruim, R. H., Mennes, M., Buitelaar, J. K., and Beckmann, C. F. (2015). Evaluation of ICA-AROMA and alternative strategies for motion artifact removal in resting state fMRI. *NeuroImage*, 112:278–287.

Salimi-Khorshidi, G., Douaud, G., Beckmann, C.F., Glasser, M.F., Griffanti, L., and Smith, S.M. (2014). Automatic denoising of functional MRI data: Combining independent component analysis and hierarchical fusion of classifiers. *NeuroImage*, 90:449–468.